14th International Conference on Applications of Statistics and Probability in Civil Engineering, ICASP14
Dublin, Ireland, July 9-13, 2023

Probabilistic Seismic Drift Demand on SMRF based on Extended Modal Analysis and Natural-Period-dependent Spectrum Intensity

Yasuhiro Mori
Professor, Dept. of Environmental Engineering and Architecture, Nagoya University, Nagoya, Japan

Kazuki Izumi
Graduate Student, Dept. of Environmental Engineering and Architecture, Nagoya University, Nagoya, Japan

Taishi Furukawa
Senior Research Engineer, Reliability Consultancy Inc., City, Country

ABSTRACT: The objective of this study is to develop a simple framework for estimating the probabilistic seismic demand of an SMRF for use in seismic-performance assessment and design. The previously proposed methods for predicting the responses of the SMRF to a given ground motion and estimating the maximum displacement response, $d_{\max}$, of the inelastic oscillator equivalent to the first mode are extended by using uniform hazard spectral intensity for the CDF of $d_{\max}$ and uniform hazard spectrum for modal combination to take the probabilistic seismic hazard information into the framework.

1. INTRODUCTION

Seismic demand such as the peak inter-story drift ratio (ISDR) of a structure should be estimated precisely in a probabilistic manner to realize an appropriate structural seismic-performance design and assessment. As a simple tool for predicting or estimating the seismic response of a two-dimensional frame to a ground motion with less required computational time than a nonlinear dynamic analysis (NDA), several methods have been proposed based on the results of a nonlinear static pushover analysis (Luco, et al. 2002; Chopra & Goel 2003; Mori et al. 2006). These methods comprise the use of the maximum displacement response, $d_{\max}$, of the inelastic oscillator, which is equivalent to the first mode of the original frame. Some of them also consider the higher modal responses and change in the post-elastic first modal shape.

In order to apply such methods in practice, the authors have developed a simple method for estimating the $d_{\max}$ of an inelastic oscillator based on natural-period-dependent spectrum intensity, SI_{μ} (Furukawa & Mori, 2020); this method is more reliable than existing techniques such as an equivalent linearization technique (ELT).

The post-elastic first modal shape changes complicated manner because of irregular formations of plastic hinges at the ends of members. To consider this problem, the authors have proposed to approximate probability distribution of the inelastic first modal response of each story by a shifted-lognormal distribution function to consider the probabilistic seismic hazard information at the construction site (Mori & Furukawa, 2021). The first modal responses of each story at three exceedance probabilities are estimated using the deflection shape of the frame corresponding to each of $d_{\max}$ as the modal shape.

The objective of this study is to develop a simple framework for estimating exceedance probability, p_{ex}, of the peak ISDR at each story of an SMRF on the basis of the above methods. The accuracy of the proposed method is investigated by comparing the p_{ex} estimated by the proposed method with the p_{ex} obtained via Monte Carlo simulations considering various seismic activities around a site and correlations among spectral accelerations.

2. OUTLINES OF PREVIOUSLY PROPOSED METHOD

2.1. *Simple method for estimating peak ISDR*

The authors have proposed Inelastic Modal Predictor (IMP, Mori et al. 2006) as a simple method for estimating the peak ISDR of an SMRF. IMP can be described as an application of the commonly used square root of the sum of the squares (SRSS) method for modal decomposition and superposition analysis using response spectra but with the inelastic first modal response; that is, the first-modal elastic spectral displacement $S_d^E(T_1, h_1)$ is replaced with the first-modal inelastic spectral displacement $S_d^I(T_1, h_1) = d_{\max}$, and the first-modal elastic vector $\phi_{1,i}^E$ is replaced with the first-modal inelastic vector $\phi_{1,i}^I$.

On considering the modes up till the s-th mode, the predictor of the peak ISDR for the i-th story, $\hat{\theta}_i$, can be evaluated as

$$\hat{\theta}_i = \sqrt{\left\{PF_{1,i}^I \cdot S_d^I(T_1; h_1)\right\}^2 + \sum_{j=2}^{s}\left\{PF_{j,i}^E \cdot S_d^E(T_j; h_j)\right\}^2} \quad (1)$$

where $S_d^E(T_j; h_j)$ is the j-th modal elastic spectral displacement, and $PF_{j,i}^E$ is the participation function of the ISDR of the j-th mode defined as

$$PF_{j,i}^E = \Gamma_j^E \frac{\phi_{j,i}^E - \phi_{j,i-1}^E}{H_i} \quad (2)$$

where $\phi_{j,i}^E$ is the element of the j-th modal vector that corresponds to the upper floor of the i-th story, H_i is the height of the i-th story, and Γ_j^E is the participation factor of the j-th mode.

The participation function $PF_{1,i}^I$ of the first mode after yielding in Eq.(1) is evaluated using Eq.(2) with $\phi_{1,i}^E$ replaced by $\phi_{1,i}^I$. Here, it is assumed that $\phi_{1,i}^I$, can be approximated by the deflected shape of the frame at a certain step in an incremental nonlinear static pushover analysis of the frame with a lateral load pattern proportional to the design load used in Japanese regulations (Midorikawa, et al. 2003) and considering P-Δ effect. The step number in the pushover analysis is determined so that the roof drift, d_{roof}, at the step corresponds to the $d_{\max}$ of the inelastic oscillator equivalent to the frame. By matching the backbone curve of the oscillator with the base shear versus d_{roof} relation obtained from the pushover analysis the corresponding d_{roof} can be determined for each ground motion.

2.2. *Simple method for estimating d_{max}*

2.2.1. *Natural-period-dependent spectral intensity*

In order to apply IMP in practice, a simple but accurate method for estimating $d_{\max}$ has been expected. The authors have proposed an estimation method of $d_{\max}$ based on natural-period-dependent spectral intensity, SI_μ (Kitahara & Itoh 2000), which is newly defined here as

$$SI_\mu = \int_{T_1}^{T_{\text{el}}} S_{\text{a}}(T; h_1)\mathrm{d}T \quad (3)$$

Using the secant stiffness at $d_{\max}$, the elongated natural period T_{el} of oscillators with bi-linear, bi-linear-slip, or tri-linear hysteresis curves can be estimated as a function of the maximum ductility factor $\mu = d_{\max}/d_{\text{y}}$, where d_{y} is the yield displacement of an oscillator. Figure 1 presents the relationship between the shear force Q and displacement d of the oscillators with (a) bi-linear, bi-linear-slip, and (b) tri-linear hysteresis curve. Here, m is the mass; $\mu_{\text{g}} = d_{\text{y2}}/d_{\text{y}}$; k is the elastic stiffness; k_{g} is the secant stiffness connecting the origin and second break point; C_{y2} is the shear force coefficient at the second break point; T_{g} is the natural period based on k_{g}; and α and $\alpha\beta$ are the second and third slopes of the stiffness, respectively.

2.2.2. *Relationship between SI_μ and $d_{\max}$*

On the basis of a number of the nonlinear dynamic analyses (NDA) of inelastic oscillators with bi-linear, bi-linear-slip, or tri-linear hysteresis curves, various natural periods, yield shear coefficient, and second or third stiffness ratio and using a number of ground motion records, the authors found that close to linear relationship between $\ln(SI_\mu)$ and $\ln(d_0)$ for $\mu = d_{\max}/d_{\text{y}} < 20$ as show in by ● in Figure 2. σ_{SI}'s in Figure 2 are

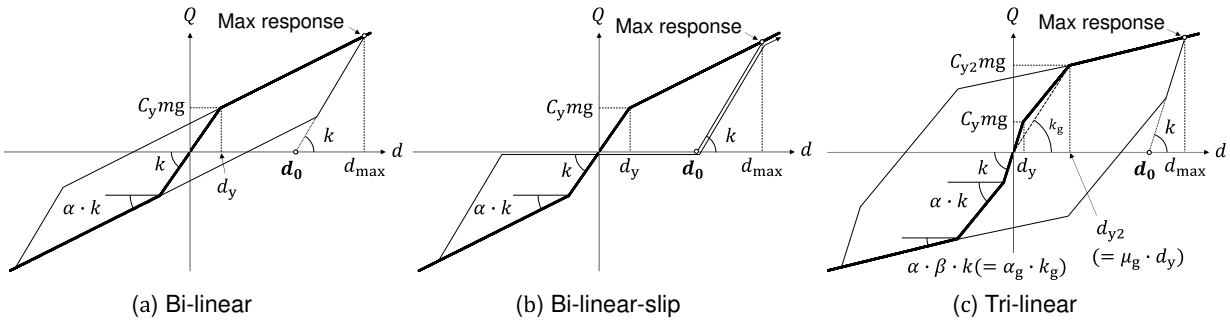

Figure 1: Parameters of hysteresis curve

the dispersions of the results along the regressed line. Here, d_0 is the interception of $Q = 0$ and the linear line with a slope of k though the maximum response point, as shown in Figure 1, and defined by the following equation.

$$d_0 = \begin{cases} [\textbf{Bi-linear},\ \textbf{Bi-linear-slip}] \\ d_y(\mu - 1)(1 - \alpha) \\ [\textbf{Tri-linear}] \\ \begin{cases} d_y(\mu - 1)(1 - \alpha); (\mu \le \mu_g) \\ d_y(\mu - 1)(1 - \alpha) + d_y(\mu - \mu_g)(\alpha - \alpha\beta); (\mu > \mu_g) \end{cases} \end{cases} \quad (4)$$

The relationship can be modeled as

$$\ln(d_0) = b_1 \cdot \ln(SI_\mu) + b_2 + \varepsilon \quad (5)$$

where ε is the error term. On the basis of regression analysis, b_1 and b_2 in Eq.(5) can be estimated using Eqs. (6) and (7), respectively.

$$b_1 = c_1 \cdot \ln(T_1) + c_2/T_1 + c_3 \quad (6)$$

$$b_2 = c_4 \cdot \ln(T_1) + c_5 \quad (7)$$

The values of the parameters c_i's in Eqs.(6)-(8) can be found in Mori & Furukawa (2021).

2.2.3. *Estimation method for d_{max}*

The d_{max} of an inelastic oscillator subjected to a ground motion can be estimated as the intersection of the straight line modeled by Eq. (5) (solid line in Figure 3) and the relationship between SI_μ and d_0 of the ground motion (dashed line in Figure 3), referred hereafter to as the "spectrum line." The spectrum line of a ground motion can be drawn by repeating the following calculations: (1) assume a value for μ, (2) substitute the μ value in Eq.(4) for d_0, and (3) substitute T_{el} in Eq. (3)

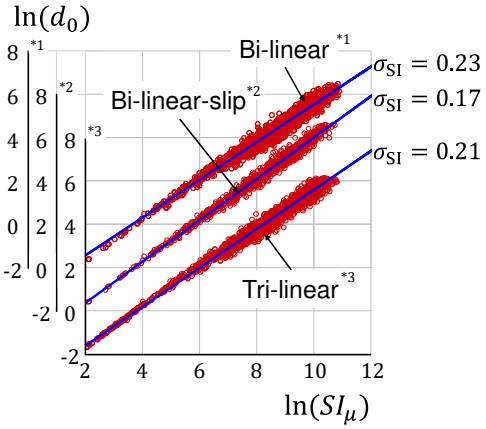

Figure 2: Relationship between $\ln(SI_\mu)$ and $\ln(d_0)$ of oscillator with each hysteresis curve

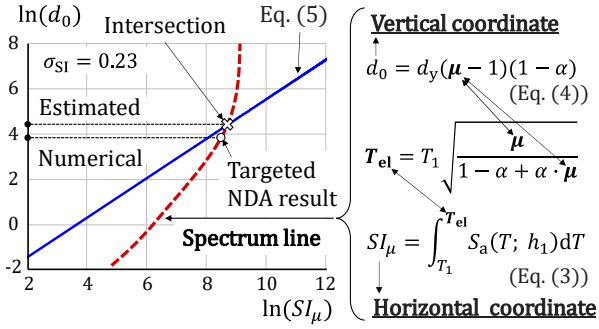

Figure 3: Estimation method for maximum displacement response

for SI_μ of the ground motion. In Figure 3, the NDA result of an oscillator for a given ground motion (outlined circle) is also presented. By definition, the NDA result is always located on the spectrum line of a given ground motion.

The accuracy of various estimation methods can be examined based on their bias, a, which is defined as the median of the ratio between the

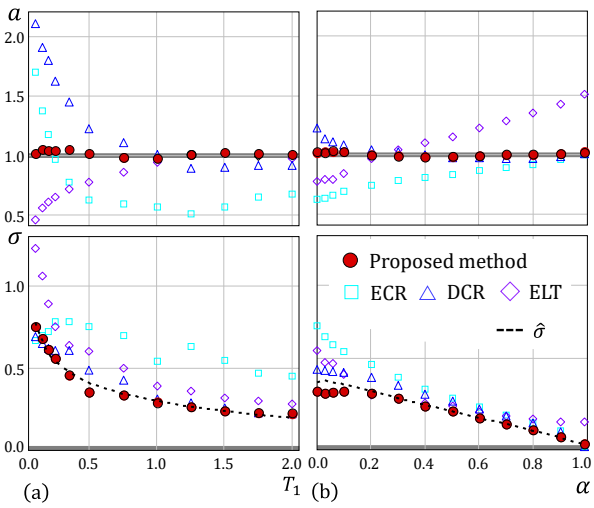

Figure 4: Comparison of bias and dispersion (bi-linear; (a) $\alpha = 0.00$ and (b) $T_1 = 0.50$)

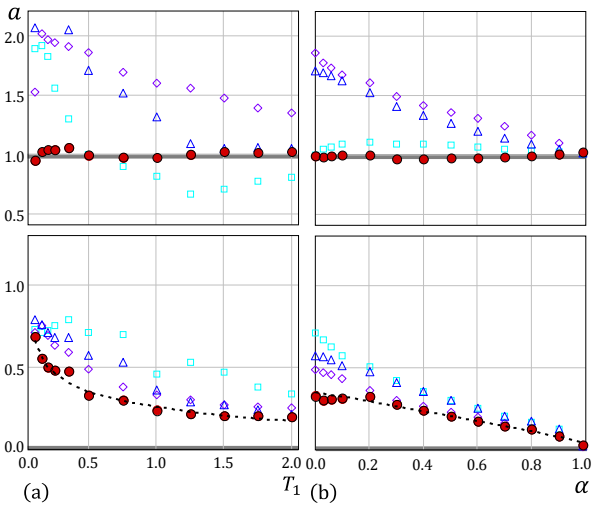

Figure 5: Comparison of bias and dispersion (bi-linear-slip; (a) $\alpha = 0.00$ and (b) $T_1 = 0.50$)

estimate, μ_{est}, and the μ value calculated via the NDA, μ_{NDA}, for each ground motion record, and its dispersion σ, which is defined by the standard deviation of the natural logarithms of $\mu_{\text{est}}/\mu_{\text{NDA}}$.

Figures 4 and 5 present the bias a in the upper figures and dispersion σ in the lower figures of the estimators by the results of the energy conservation rule (ECR), displacement conservation rule (DCR), equivalent linearization technique (ELT), and the proposed method, (a) as a function of T_1 of the oscillators with a bi-linear (Figure 4) or bi-linear-slip (Figure 5) hysteresis curve of $\alpha = 0.00$, and (b) as a function of α of

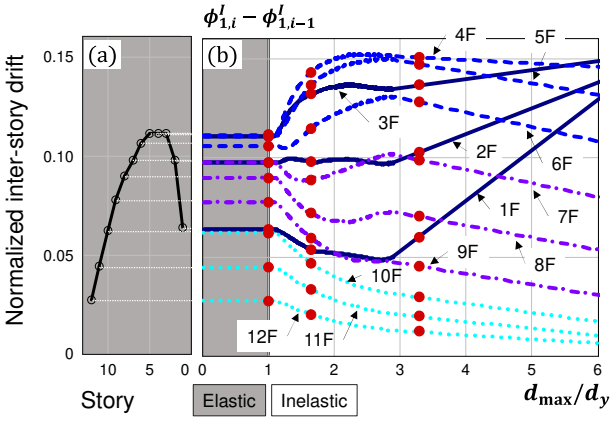

Figure 6: (a) Normalized inter-story drift; and (b) Relationship between $\phi^I_{1,i} - \phi^I_{1,i-1}$ and d_{max}/d_y

the oscillators with $T_1 = 0.50$. It can be found that in the proposed method, the bias, a, of is approximately equal to unity for all of the oscillators. In addition, in this method, σ is smaller than or approximately equal to those of the other methods.

The dashed line in the lower part of Figures 4 and 5 indicates the dispersions σ of the proposed method, which can be modeled as

$$\hat{\sigma} = c_6 \cdot \ln(T_1) + c_7/T_1 + c_8 \qquad (8)$$

2.3. *Exceedance probability of first modal responses*

Assume for now that the CDF of $d_{\max}$ is available. When estimating the probability distribution of the inelastic first modal response at each story of an SMRF on the basis of the CDF of $d_{\max}$ (Eq.(1)), it is necessary to take into consideration the change in the shape of the modal response $\phi^I_{1,i}$ depending on the intensity of $d_{\max}$ of the inelastic oscillator equivalent to the first mode. Figure 6 presents an example of (a) inter-story drifts in elastic range of a six-bay 12-story building used in the numerical examples in Section 4 and (b) the values of the elements of the inelastic first modal vector in the form of $(\phi^I_{1,i} - \phi^I_{1,i-1})$ as a function of the maximum ductility factor of the equivalent inelastic oscillator μ. Note that here the story drifts are normalized so that the roof drift d_{roof} is unity. The shaded area in the figure indicates the range of elastic response. The solid lines, dashed lines, and chain lines in Figure

6(b) indicate the $\phi^{\bullet}_{1,i}$ values of stories 1 - 4, stories 5 - 8, and stories 9 - 12, respectively. As can be observed in Figure 6(b) that $(\phi^{I}_{1,i} - \phi^{I}_{1,i-1})$ changes in complexity with $d_{\max}$, and thus, the probability distribution of the inelastic first modal response of each story also changes in complexity. Based on such observations, it is proposed here the inelastic first modal response of the i-th story, $\hat{X}_i$, be approximated to a shifted-lognormal random variable. By using a three parameter random variables, better approximation of p_{ex} can be achieved than using a two parameter random variable.

The cumulative distribution function (CDF) of a shifted-lognormal random variable X, $F_X(x)$, can be expressed as

$$F_X(x) = \Phi\left(\frac{\ln(x - x_0) - \mu_{\ln Y}}{\sigma_{\ln Y}}\right) \qquad (9)$$

where $\Phi(\cdot)$ is the standard normal CDF; $\mu_{\ln Y}$ and $\sigma_{\ln Y}$ are the mean and standard deviation, respectively, of $\ln Y$; and Y is a log-normal random variable defined as $Y = X - x_0$.

A random variable $\tilde{X}$ can be approximated as a shifted-lognormal random variable X such that the CDF of $\tilde{X}$, $F_{\tilde{X}}(x)$, is equal to that of X, at three exceedance probabilities p_k ($k = 1,2,3$, and $p_1 > p_2 > p_3$), and the parameters $\mu_{\ln Y}$, $\sigma_{\ln Y}$, and x_0 in Eq.(9) can be obtained as follows:

$$F_{\tilde{X}}(x_k) = F_X(x_k) = 1 - p_k = \Phi(a_k) \qquad (10)$$

Under the conditions that

$$a_1 = a_0, \quad a_2 = a_0 + b_0, \quad \text{and} \quad a_3 = a_0 + 2b_0 \qquad (11)$$

then the nonlinear simultaneous equations (Eq.(10)) can be solved analytically as

$$x_0 = \frac{x_1 \cdot x_3 - {x_2}^2}{x_1 + x_3 - 2 \cdot x_2} \qquad (12)$$

$$\sigma_{\ln Y} = \ln\left\{\left(\frac{x_3 - x_2}{x_2 - x_1}\right)^{1/b_0}\right\} \qquad (13)$$

$$\mu_{\ln Y} = \ln\left\{\frac{(x_2 - x_1)^2}{x_1 + x_3 - 2 \cdot x_2}\right\} - a_0 \cdot \sigma_{\ln Y} \qquad (14)$$

It should be noted that $x_1 + x_3 - 2x_2 > 0$.

When approximating the inelastic modal response at the i-th story, $\hat{X}_i$, to a shifted-lognormal random variable X_i, p_1 in Eq.(10) is set as the probability that the equivalent inelastic oscillator yields, p_{y}, which can be estimated from the probability distribution of elastic spectral displacement, and p_3 is set to the minimum exceedance probability considered in the design and assessment. a_0 and b_0 in Eq.(11) can be obtained by substituting Eq.(11) into Eq.(10).

$$\begin{cases} a_0 = \Phi^{-1}(-p_{\text{y}}) \\ b_0 = \{-a_0 + \Phi^{-1}(-p_3)\}/2 \end{cases} \qquad (15)$$

Then p_2 is determined as

$$p_2 = \Phi(-\{a_0 + \Phi^{-1}(-p_3)\}/2) \qquad (16)$$

The parameters of the CDF of X_i can be determined by substituted the peak ISDR, $\theta_{i,k}$, of which exceedance probability is equal to p_k ($k = 1,2,3$) into x_k as per Eqs.(12), (13), and (14).

$\theta_{i,k}$ is determined by the following equation, which corresponds to the first term in the right-hand side of Eq.(1).

$$\theta_{i,k} = PF^{I}_{1,i,k} \cdot d_{\max,k} \qquad (17)$$

where $d_{\max,k}$ is the response of the equivalent inelastic oscillator corresponding to $p_{\text{ex}} = p_k$, which will be discussed in Section 3. $PF^{I}_{1,i,k}$ in Eq.(17) is estimated by Eq.(2) with $\phi^{E}_{j,i}$'s are replaced by the inelastic first modal vector approximated by the deflection shape from nonlinear static pushover analysis at the step d_{roof} corresponds to $d_{\max,k}$.

3. SIMPLE FRAMEWORK FOR ESTIMATING p_{ex} OF PEAK ISDR

In order to extend those previously proposed methods described in Section 2 as a practical framework for estimating the probabilistic seismic demand of a structure for use in reliability-based seismic-performance assessment and design, simple tools/ideas that can take probabilistic seismic hazard information into the framework are required to be developed.

3.1. Uniform hazard spectral intensity for estimating p_{ex} of d_{max}

ELT is often used in practice to estimate $d_{\max}$ as seismic demand for structural design, and design spectra are being developed on the basis of probabilistic approaches such as a uniform hazard spectrum (UHS) and a conditional mean spectrum (CMS, Baker 2011). A UHS is obtained by plotting the response with the same exceedance probability for a suite of elastic oscillators with different natural periods, and hence, a UHS does not represent any specific ground motion (Abrahamson 2006). Although there exists some correlation among the spectral responses of elastic oscillators to a ground motion (e.g., Baker & Jayaram 2008), perfect correlation is implicitly assumed in the use of a UHS. In such a scenario, the response could be overestimated via ELT when a very rare event is considered.

The correlation among the spectral responses could be considered by using a CMS, which is the mean spectrum conditional to the event that the spectral displacement of an elastic oscillator with a certain natural period, T_c, equals the displacement with, say, 10% exceedance probability in 50 years. However, it would provide fairly optimistic estimates because the other possible events with 10% exceedance probability in 50 years are ignored (Mori, et al. 2011).

In order to overcome such issue of correlation, it is proposed here to use uniform hazard spectral intensity (UHSI), which is the natural-period-dependent spectral intensity with the same exceedance probability. Unlike spectral responses, correlation among SI_μ's with various integration rages would be fairly high. Using UHSIs with p_{ex} equal to p_1, p_2, and p_3, p_{ex} of $d_{\max}$ can be estimated by the methods described in Sections 2.2 and 2.3.

3.2. Uniform hazard spectrum for Modal combination

The SRSS method, which is the basis of Eq.(1), is often used as a simple method of combining modal responses of a structure. Originally, SRSS and also Eq.(1) were proposed for estimating the maximum response of a structure to "a ground motion." Here, it is proposed to estimate the maximum responses during certain period of time by Eq.(1) using $S_d^I(T_1; h_1)$ and $S_d^E(T_j; h_j)$'s with the same p_{ex} equal to p_1, p_2, and p_3. $S_d^E(T_j; h_j)$'s with these p_{ex}'s can be obtained from uniform hazard spectra.

4. NUMERICAL EXAMPLES

Using a probabilistic seismic hazard model, the accuracy of the p_{ex} of the peak ISDR of each story as approximated by the proposed method is investigated by comparing with the results of the Monte Carlo simulation.

4.1. Building models

Two two-dimensional SMRF buildings designed according to Japanese practice with reasonably well-balanced story-yield strengths and story-stiffness distributions are considered: (a) a five-bay six-story building denoted as 6F model and (b) a six-bay twelve-story building denoted as 12F model (Furukawa et al. 2019). Rayleigh damping is assumed for both models. Table 1 shows the natural periods and damping factors of these models up to the 3rd mode. Table 2 shows the properties of the inelastic oscillators equivalent to the 1st mode of each of the SMRF models.

Table 1: Natural periods and damping factors of building models up to 3rd mode

Model	Natural period (s)			Damping factor		
	1st	2rd	3rd	1st	2rd	3rd
6F	1.23	0.407	0.228	0.02	0.02	0.03
12F	2.17	0.722	0.41	0.02	0.02	0.029

Table 2: Properties of inelastic oscillators equivalent to building models

Model	T_1 (s)	h_1	d_y (mm)	d_{y_2} (mm)	α	$\alpha\beta$
6F	1.23	0.02	158.4	525.4	0.06	0
12F	2.17	0.02	357.0	836.7	0.08	0

4.2. Probabilistic Seismic hazard model

It is assumed that

- Within a square area with side length equal to 300 km, earthquakes with the magnitude greater than 5.0 occur following Poisson process in time and space with annual mean occurrence rate equal to 8/3.

- The site for estimating the seismic hazard locates at the center of the square area.
- The magnitude of an earthquake follows Gutenberg-Richiter relationship with parameter b equal to 1.25 and the upper limit of magnitude equal to 9.0.
- In addition to randomly occurring earthquakes, an interpolate earthquake could occur with magnitude following normal probability distribution with mean equal to 8.4 and standard deviation equal to 0.2. The fault locates 60 km away from the site. The recurrence period of the earthquake follows BPT distribution with mean equal to 300 years and coefficient of variation equal to 0.25. It is further assumed that 210 years has passed since the last activity of the fault.
- The acceleration response spectrum with 5 % damping at the engineering bedrock at the site owing to an earthquake is estimated by the regression formula proposed by Morikawa & Fujiwara (2013) with increments of 0.01 s. The correlations among the spectral responses are considered (Baker & Jayaram 2008).
- The acceleration response spectrum, $S_a(T)$, on the surface is estimated by considering the soil amplification factor of medium soil (soil type 2) prescribed in the Japanese regulation (Midorikawa et al. 2003).

4.3. *Exceedance probability of peak ISDR*

One-thousand samples of a 50-year seismic activity are generated. More than one earthquake could occur during a single 50 years; those earthquakes with PGV less than 50 mm/s at the site are excluded for the sake of the efficiency of the analysis.

For each sample of 50 years, the maximum $S_a(T)$ during the period is found for each natural period with increment of 0.01 s. Then the CDFs of the maximum $S_a(T)$ in 50 years are estimated. A uniform hazard spectrum can be obtained by connecting the values with the same exceedance probability of these CDFs.

Also, the SI_μ of each ground motion for the 6F model and 12F model are estimated at each natural period by integrating its $S_a(T)$ from the first natural period of the respective model to the upper limit of the integration with increment of 0.01 s. Then for each sample of 50 years, the maximum SI_μ during the period is found for each of the upper limit of the integration. The CDFs of the SI_μ for the 6F model and 12F model are estimated on the basis of these maximum SI_μ's. A UHSI can be obtained by connecting the values with the same exceedance probability.

Figures 7 and 8 show the p_{ex} in 50 years of the peak ISDR at each story of the 6F model and 12F model, respectively, estimated by the proposed method considering up to the third modal responses (solid lines). In the proposed method, p_1 in Eq.(10) is determined as the probability that the equivalent oscillator yields on the basis of the probability distribution of $S_a(T_1)$, and p_3 is set to be 0.02. Then applying the method

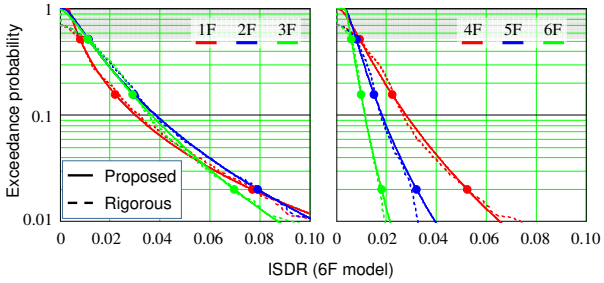

Figure 7: Exceedance probability of ISDR of 6F

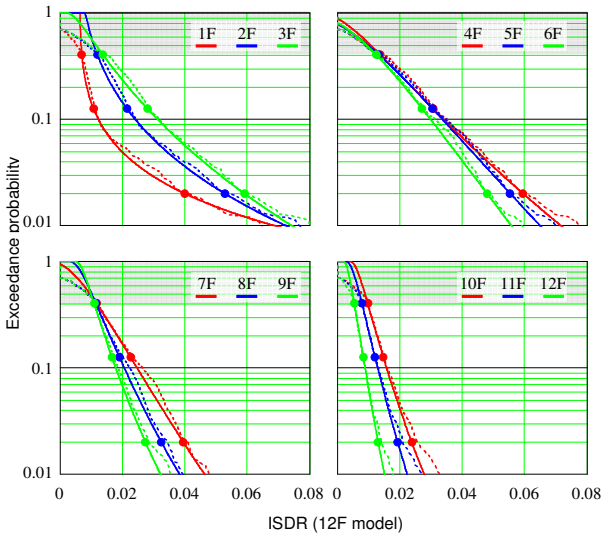

Figure 8: Exceedance probability of ISDR of 12F

described in 2.1.1, $S_d^I(T_1; h_1)$ corresponding to p_1, p_2, and p_3 can be estimated. The elastic responses of the oscillator equivalent to higher modes $S_d^E(T_j; h_j)$ $(j = 2, 3)$ corresponding to p_1, p_2, and p_3 are estimated from the CDFs of $S_a(T_j)$ using damping correction factors (Kasai et al. 2003). These spectral displacements are substituted in Eq.(1) to obtain the peak ISDR of each story corresponding to p_1, p_2, and p_3, which are shown by ● in the figures. Then, the p_{ex} in 50 years are approximated by a shifted log-normal distribution function.

In Figures 7 and 8, more rigorous results are also presented (dashed lines). In the rigorous analysis, $S_d^I(T_1; h_1)$ is estimated for each ground motion generated in the simulation by the method described in 2.1.2, and the peak ISDR owing to the ground motion is estimated by Eq.(1). The p_{ex} in 50 years are estimated on the basis of the maximum peak ISDR during each sample of 50 years. It can be observed that p_{ex}'s by the proposed method in Figures 7 and 8 are very close to those by the rigorous analysis at all stories of both 6F and 12F models.

5. CONCLUSIONS

In this study, a framework for estimating the probabilistic seismic demand of an SMRF for use in reliability-based seismic-performance assessment and design is presented. The previously proposed methods for (1) predicting the responses for a given ground motion considering the inelastic response of the inelastic oscillator equivalent to the first mode and change in the first modal shape after yielding, (2) estimating $d_{\max}$ of the equivalent oscillator using the natural-period-dependent spectral intensity of a ground motion, and (3) approximating the p_{ex} of the inelastic first modal response of each story by a shifted-lognormal distribution function are extended with the use of uniform hazard spectral intensity for the CDF of $d_{\max}$ and uniform hazard spectra for modal combination to take the probabilistic seismic hazard information into the framework. The accuracy of the proposed framework is investigated using numerical examples.

6. REFERENCES

Abrahamson, N., 2006. "Seismic hazard assessment: problems with current practice and future developments," *Proc. 1st European Conf. on Earthquake Engrg. & Seismology*, Geneva, Switzerland, 1-17.

Baker, J.W. and C.A. Cornell, 2006. "Correlation of response spectral values for multi component ground motion," *Bulletin of the Seismological Society of America*, 96(1), 215-227.

Baker, J.W. and Jayaram, N. 2008. "Correlation of spectral acceleration values from NGA ground motion models," *Earthquake Spectra*, 24(1): 299-317.

Baker, J.W. 2011. "Conditional mean spectrum: tool for ground-motion selection," *J. Structural Engrg.*, 137(3): 322-331.

Furukawa, T., Mori, Y., and Kang, J. D. 2019. "Maximum response estimation method of an oscillator based on natural period-dependent spectrum intensity," *Proc. 13th Int. Conf. on Applications of Statistics & Probability in Civil Engrg*.

Furukawa, T. and Mori, Y. 2020. "Simplified method for estimating maximum displacement of inelastic oscillator based on natural period-dependent spectrum intensity," *J. Structural & Construction Engrg.*, 773: 869-878. (in Japanese)

Kasai, K., Ito, H., and Watanebe, A. 2003. "Peak response prediction rule for a SDOF elasto-plastic system based on equivalent linearization technique," *J. Structural & Construction Engrg.*, 571: 53-62. (in Japanese)

Kitahara, K. and Itoh, Y. 2000. "Correlation between nonlinear response of bridge piers and natural-period-dependent spectrum intensity," *Proc. 12 WCEE*, Paper No. 0806.

Midorikawa, M., Okawa, I., Iiba, M., and Teshigawara, M. 2003. "Performance-based seismic design code for buildings in Japan," *Earthquake Engrg. & Engrg. Seismology*, 4(1): 15-25.

Mori, Y., Yamanaka, T., Luco, N., and Cornell, C. A. 2006. "A static predictor of seismic demand on frames based on a post-elastic deflected shape," *Earthquake Engrg. & Structural Dynamics*, 35: 1295-1318.

Mori, Y. & Furukawa, T., 2021. "Probabilistic predictor of seismic demand on SMRF based on natural-period-dependent spectrum intensity," *Structural Safety,* 89: 102040.

Morikawa, N. & Fujiwara, H., 2013. "A New ground motion prediction equation for japan applicable up to M9 mega-earthquake," *J. of Disaster Research*, 8(5): 878-888.